Int J Adv Manuf Technol (2000) 16:822–829

The International Journal of
Advanced
Manufacturing
Technology

Flexible Fixturing with Phase-Change Materials. Part 1. Experimental Study on Magnetorheological Fluids

Y. Rong[1], R. Tao[2] and X. Tang[2]

[1]Department of Mechanical Engineering, Worcester Polytechnic Institute, Worcester, USA; and [2]Department of Physics, Southern Illinois University at Carbondale, Carbondale, USA

Flexible fixturing is an important issue in manufacturing, where a single set of fixtures are used for locating and holding a variety of workpieces. Flexible fixturing with phase-change materials involves the use of functional materials which change the status from liquid to solid under certain conditions. The workpiece is located in the liquid fixture material and held firmly when the material is changed into the solid state. Therefore, the material strength in the solid state is crucial for a successful application to production.

This paper presents an experimental study of magnetorheological (MR) fluid material. With the application of a compression technique, a thick column structure is formed and enhanced. Hence, a high shear strength of the MR fluid in solid status is achieved. Experimental results are reported in this paper. Further application of this technique is under development for flexible fixturing in industrial applications.

Keywords: Flexible fixturing; Flexible manufacturing systems; Magnet orheological fluid

1. Introduction

Recently, there is a great deal of interest in flexible fixturing, which involves employing a single device to hold parts or assemblies of different shapes and sizes while they are being subjected to a wide variety of external force fields and torques associated with conventional manufacturing operations. Currently, the most widely used flexible fixtures are adjustable fixtures and modular fixtures [1,2]. The former is specially designed for a family of parts. Through adjustments of the positions of one or more fixture elements (locators and/or clamps), a certain degree of flexibility can be expected. Modular fixtures were originally developed for small batch production to reduce the fixturing cost, where a dedicated fixture was not economically feasible. The flexibility of a modular fixture is derived from the large number of fixture configurations from different combinations of the fixture elements which may be bolted to a baseplate. Computer-aided fixture design (CAFD) technique has been rapidly developed in recent years in order to apply modular fixtures in industry widely [3,4]. Problems involved in the application of adjustable and modular fixtures include the limitation of flexibility which may not be suitable for irregular shaped workpieces such as turbine blades. The concentrated clamping forces may lead to undesired deformation, especially in precision machining of parts with complex geometry. The large number of fixture elements stored to ensure the flexibility by different combinations also results in an increase of work-in-process inventory.

Flexible fixturing based on the concept of material phase-change exploits the ability of certain classes of materials to change from a fluid to a solid, and back to a fluid again, which has become one of the most promising technologies in flexible fixturing [5]. This phase-change must be easy to control and must have no harmful effect on the workpiece. Typical operations in applying this type of fixture include two steps. First, when the material is in the fluid state, the workpiece is immersed in the fluid. By altering certain conditions, the fluid is changed to a solid which holds the workpiece fixed. Then, the workpiece is subjected to the desired operation. After the operation, the workpiece can be removed from the fixture by changing the material back into a fluid.

Fixtures with phase-change materials can be broadly classified into two groups:

1. Fixtures incorporating materials which undergo an authentic phase-change.
2. Fixtures incorporating materials which undergo a pseudo-phase-change [6].

In an authentic phase-change, temperature has been used to control the change [7]. Up to now, low-melting-point alloys are most widely employed for phase-change fixtures. However, the temperature change may cause deformations, because the wall thickness of the workpieces may be different and the speeds of phase change may vary. Therefore, low-melting-point alloys have limitations when used for flexible fixtures. There

Correspondence and offprint requests to: Professor Y. Rong, Department of Mechanical Engineering, Worcester Polytechnic Institute, 100 Institute Road, Worcester, MA 01609-2280, USA. E-mail: rong@wpi.edu

are also serious environmental concerns over the presence of the element lead in low-melting-point alloys.

A fixture with pseudo-phase-change materials uses the two-phase nature of a particulate fluidised bed. A container (fluid-bed) is filled with particles and incorporates a porous floor through which a stream of air passes at a carefully controlled rate. When the air supply is activated, the particulate bed acts as a fluid, permitting the workpiece to be placed into the bed with minimal resistance. The air supply is then switched off and the particles compact under gravitational loading to form a solid mass which holds the workpiece in place. The workpiece is then subjected to the desired sequence of operations. After the operations, the workpiece is unloaded by reactivating the air supply [8,9]. Although the phase of the materials is not changed in these processes, the fixturing principle is very similar to phase-change fixturing. However, the magnitude of the force that can be exerted on the part is limited in these pseudo-phase-change materials. Clamping stability could be a problem when the workpieces are subjected to strong machining forces.

Fixtures using phase-change materials can be adapted easily to the change of part geometry. Therefore, phase-change fixtures are a type of truly flexible fixture. In contrast to mechanical fixturing, in which the clamping forces are applied only on very small areas, even points, phase-change fixturing has the ultimate conformity of forces. It is suited for workpieces with complex curved surfaces which must be held during operations and the workpieces which are compliant and are liable to deform. The development of flexible fixtures with phase-change materials presents great potential for innovation in flexible fixturing technology.

2. Electrorheological and Magnetorheological Fluids

Electrorheological (ER) and magnetorheological (MR) fluids are typical phase-change materials where electrical and magnetic fields are applied to control the phase-change. A typical ER fluid is made of a suspension of fine dielectric particles in a liquid of low dielectric constant [10,11]. If there is no electrical field (E) applied, the liquid suspension is stable with low viscosity. When E is applied, there are two kinds of interaction, first, between dielectric particles and electrical field, and, secondly, between the dielectric particles. The effective viscosity increases dramatically as E increases. Once E exceeds a critical value, the ER fluid becomes a solid with a body-centred tetragonal (BCT) structure. Figure 1 shows the dielectric particle distributions at different stages of applying the electrical field [11]. Figure 2 shows experimental measurement of the BCT structure [12]. The yield stress increases as E is further strengthened. This process is reversible with a transition time of less than 1 ms. Since a phase-change in ER materials is induced by an electric field, the ER effect covers a wide range of temperatures and need not cause temperature changes in the workpiece. In addition, an induced ER solid is much stronger than a system with close-packed particles under earth gravity, employed in pseudo-phase-change fixtures. Current ER fluids have a typical yield stress of around 10 kPa and the highest is about 60 kPa [13]. Therefore, ER materials can be ideal for flexible fixturing: strong, totally flexible, and quick in operation. Since a strong electric field is required to induce the phase-change, the ER fluid is usually applied as a thin film to minimise the distance between the two poles.

Similarly, MR fluids consist of a suspension of ferromagnetic or paramagnetic particles of micrometre size in a non-magnetic carrier fluid. Surfactants are added to alleviate the settling problem. When a magnetic field is applied, the particles become polarised and are thereby arranged into chains or clusters. The chains can further aggregate into columns, when the MR fluid exhibits a solid-like mechanical behaviour. Its strength further increases with the external field. Field-induced solidification is reversible and the timescale for the chain formation is in the order of milliseconds. The performance of MR fluids depends on their chemical and physical stability, temperature dependence, zero-field viscosity, response time, and the yield stress. Among these factors, the yield stress, being an indication how strong MR fluids are in a magnetic field, is the key parameter for applications, especially in flexible fixturing.

Currently, MR fluids have a typical shear stress of around 80 kPa. Therefore, MR fluids began to be employed in a few industrial applications such as shock absorbers, clutches, engine mounts, and vibration controls [14,15]. Ginder and Davis [16] predicted that the yield stress of an iron-based MR fluid at 50% volume fraction was about 200 kPa. Their calculation is based on a single-chain structure and takes the magnetic saturation into account. The prediction would be correct if the magnetic particles in MR fluids form only the single-chain structure.

ER and MR fluids have attracted considerable attention recently because the mechanical properties of these fluids can be electrically controlled. The field-induced shear stresses in MR fluids are even larger than for ER fluids in magnitude, which is especially advantageous when processing non-ferrous metals [14]. The property requirements of ER and MR phase-change materials for flexible fixturing must be satisfied, such as chemical stability (not reacting with the workpiece), phase-change property stability, fast phase-change, uniformity throughout all the material volume, and fast operation time. The mechanical characteristics of the materials are also important in flexible fixturing applications, such as strength and stiffness in the solid state, variation range of viscosity and density in the solid and fluid states, and complexity of control and operation. The shear and tensile strength and stiffness are required to be large, which implies that the viscosity of ER or MR fluids is required to be very large (larger than that required in most other applications). The zero-field viscosity is relatively less important in this specific application. It is crucial to synthesise phase-change materials with acceptable shear and tension strength in the solid state for fixturing, with a low production cost.

3. Experimental Study on Magnetorheological Fluid

It is well known now that under a strong magnetic (or electric) field, the ideal structure of MR (or ER) fluids is a BCT lattice

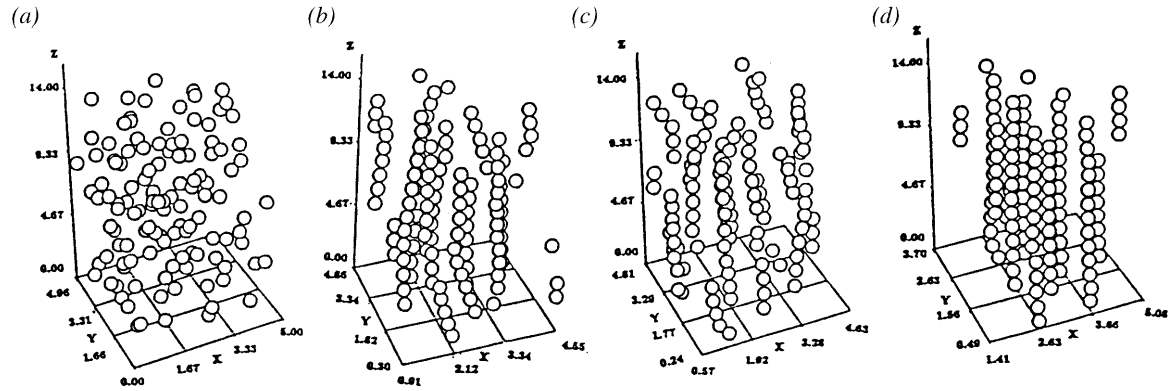

Fig. 1. BCT structure formation process. (*a*) In the initial state, dielectric particles are randomly distributed. (*b*) After 10 ms of applying a strong electric field, particles begin to move. (*c*) After 30 ms of applying a strong electric field, the lateral ordering is building. (*d*) After 180 ms of applying a strong electric field, single chains have been aggregated into a BCT lattice structure.

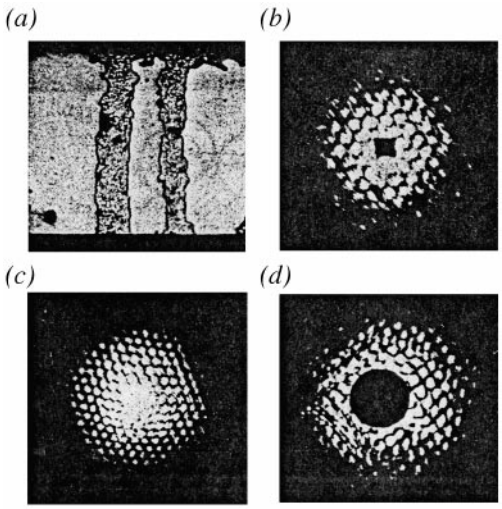

Fig. 2. BCT structure identified under microscopic views. (*a*) View of typical columns formed between the two electrodes which are separated by 3 mm. (*b*) Diffraction pattern of a (110) plane for 20.0 μm diameter spheres. (*c*) Pattern of a (110) plane for 40.7 μm diameter spheres. (*d*) Pattern of a (100) plane for 40.7 μm diameter spheres.

[17–19]. The yield stress of MR fluids strongly depends on the microstructure, i.e. the way magnetic particles are arranged in a magnetic field. For example, a BCT lattice has a much higher yield stress than a single-chain structure [20]. Experiments on steel balls with different structural arrangements also support this point [21]. Therefore, if the single-chain structure can be changed into a thick column structure, MR fluids will have a much stronger yield stress. Based on this knowledge, a new approach is sought to produce a structure with enhanced yield stress. Immediately after a magnetic field is applied, the MR fluid is compressed before a shear force is applied. The magnetic field produces particle chains in milliseconds. The compression pushes these chains together to form close-packed clusters. SEM images show that the particle chains are indeed pushed together to form thick columns. This fluid structure change greatly enhances the yield stress. Experiments on an iron-based MR fluid show this structure-enhanced static yield stress to be as high as 800 kPa, i.e. ten times the yield stress without compression. When the magnetic field is removed, the MR fluid still returns to the liquid state quickly. The upper limit of this structure-enhanced yield stress seems to be well above 800 kPa. It is expected that this method and the physical principles are also applicable to ER fluids. The super-strong MR and ER fluids developed with this method may be suitable for many applications, especially for flexible fixturing in manufacturing.

3.1 Experimental System

A suspension of carbonyl iron particles in silicone oil with a volume fraction 46–50% was used in the experiment. As shown in the SEM image (Fig. 3), the carbonyl iron particles are spherical with average diameters around 5 μm. The silicone oil has a viscosity of 0.05 poise. A small amount of surfactant was added to the suspension so that the particles remained suspended in silicon oil without settling for at least 24 hours. The zero-field viscosity was about 10 poises.

The experimental set-up is shown in Fig. 4. An electromagnet with two water-cooled coils generates a magnetic field in the horizontal direction. An aluminium container between the two magnetic poles has one sliding iron wedge and one fixed guiding iron wedge at each side, close to the magnetic

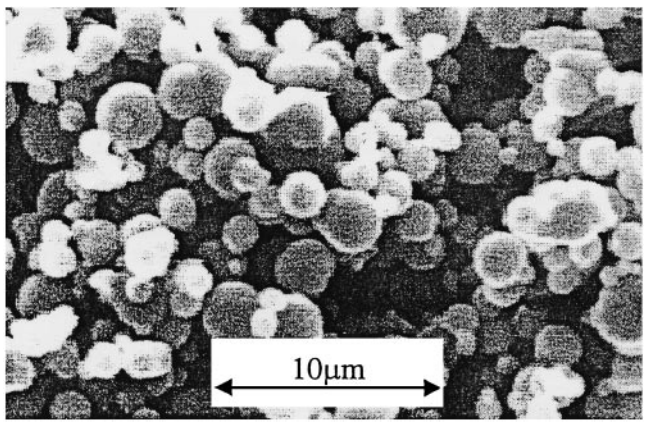

Fig. 3. SEM image of a carbonyl iron particle.

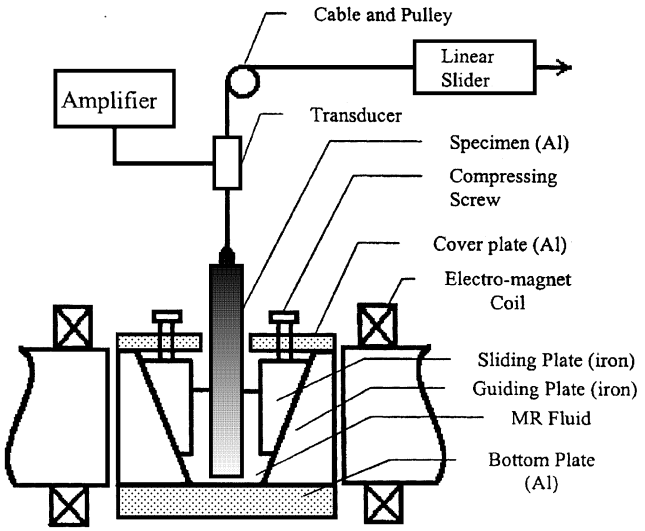

Fig. 4. The experimental set-up.

poles. The sliding plates and guiding plates are made of magnetic iron and the wall is made of aluminium alloy, which is non-magnetic. The interface between the sliding plate and the guiding plate has a 12° angle to the vertical. As the sliding wedges are pushed down, the MR fluid is compressed in the field direction. The size of the container was 89 mm × 89 mm × 115 mm, providing a volume of 200 ml. 120 ml MR fluid was poured into the container.

The experiment was performed at room temperature. Before application of the magnetic field, an aluminium test bar was inserted vertically into the centre of the container. The magnetic field was applied to solidify the MR fluid. The MR fluid was then compressed by pushing the two sliding wedges down symmetrically. When the sliding wedges were pushed down, the MR fluid level rose. Afterwards, a force was applied and gradually increased until the test bar could be pulled out. This pullout force was a function of the applied magnetic fields and the compression torque. To determine the yield stress, a force transducer with a conditioner-amplifier was used to measure the force required to pull the test bar out from the MR fluid. The MR fluid yield stress was very high in the solid state.

To determine the modulus, the vertical displacement of the bar under force was also tested. This displacement was very small before the MR fluid yielded. A small mirror was attached to the test bar. The small displacement led to a small rotation of the mirror. From a laser beam deflected from the mirror, the displacement could be determined with an accuracy of 1 μm. The displacement was so small that the tensile elongation of the test bar must be subtracted from it to obtain the correct shear strain. On the other hand, the post-yield displacement was larger. Instead of a laser beam, a mechanical micro-indicator was used to measure it.

3.2 Measured Yield Stress

The depth of the bar submerged in the MR fluid is *d*. The cross-section of the test bar is rectangular. The side perpendicular to the field is denoted as *w* and the side parallel to the field as *t*. The bottom plane $A_b = wt$. The areas perpendicular to the field and parallel to the field submerged in the MR fluid are $A_\perp = 2wd$, and $A_{//} = 2td$, respectively. The vertical force F_t required to pull out the test bar is given by

$$F_t = \tau_\perp A_\perp + \tau_{//} A_{//} + p_0 A_b + mg \quad (1)$$

where $\tau_\perp$ and $\tau_{//}$ are the yield shear stresses on a plane perpendicular to the field direction and on a plane parallel to the field direction, respectively, p_0 is the atmospheric pressure, and *mg* the weight of the test bar. The last two terms are quite small. $F_{MR} = F_t - p_0 A_b - mg = \tau_\perp A_\perp + \tau_{//} A_{//}$ is defined as the net MR pullout force. By varying the size of $A_\perp$ and $A_{//}$, $\tau_\perp$ and $\tau_{//}$ were determined. In the experiment, three aluminium bars were used, with $t = \frac{1}{2}$ in and $w = \frac{1}{2}, \frac{1}{4}, \frac{1}{8}$ in, respectively. Figure 5 shows the net MR pullout forces for the three test bars, which have the same $A_{//}$, but different $A_\perp$. *T* is the compression force on the MR fluid. It is clear that the compression leads to a much higher pullout force. It is also noted that the pullout force is almost linear with *w*, or $A_\perp$, indicating that the pullout force is mainly determined by $\tau_\perp A_\perp$. The predominant term in F_{MR} is $\tau_\perp A_\perp$.

Since the test bar is non-magnetic, the field around the bar is not uniform. The field H_1 at the front centre of the test bar was less than the field H_2 at the side parallel to the field. As it is difficult to measure the field inside the MR fluid, and the tangential component of the magnetic field is continuous at any interface that has no surface current, H_1 and H_2 are measured at the MR fluid surface. Table 1 shows H_1 and H_2 for a test bar of $t = \frac{1}{2}$ in and $w = 1$ in. As the coil current increases, the ratio H_2/H_1 drops from 1.85 at 1 A to 1.30 at 9 A. For simplicity, the average $H = (H_2 + H_1)/2$ is taken as the mean value of *H* in the calculation. Figure 6 shows F_{MR} versus the compression for a test bar of $t = \frac{1}{2}$ in and $w = 1$ in. It is clear that F_{MR} increases linearly with the compression force. Hence, the yield shear stress $\tau_{y(H)}$ increases with the normal stress P_e. An empirical expression for the yield shear stress is

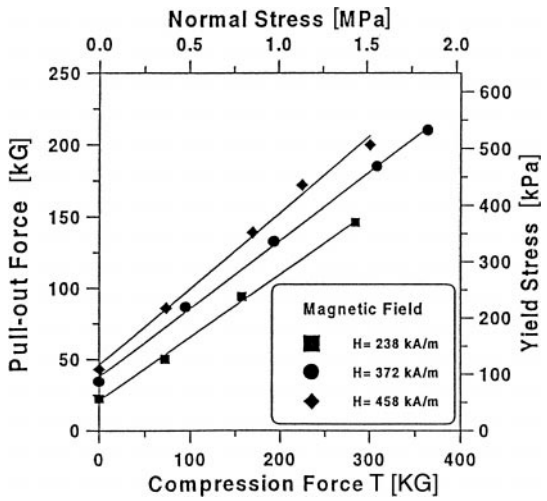

Fig. 5. Yield shear stress of the MR fluid increases with the normal stress.

Table 1. The relationship between the coil currents and the magnetic field.

Coil current I (A)	1.0	2.0	3.0	4.0	5.0	6.0	7.0	8.0	9.0
Field H_1 (kA m^{-1})	37.6	103	187	250	306	350	388	418	445
Field H_2 (kA m^{-1})	69.6	188	289	370	440	486	526	558	582
Mean field H (kA m^{-1})	53.6	146	238	310	373	418	458	488	514
Ratio H_2/H_1	1.85	1.82	1.54	1.48	1.44	1.39	1.36	1.34	1.31

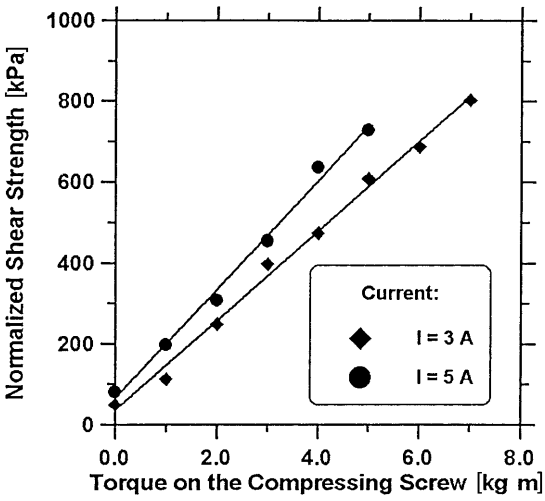

Fig. 6. The relationship between the yield shear stress and the compression pressure measured by the compression torque.

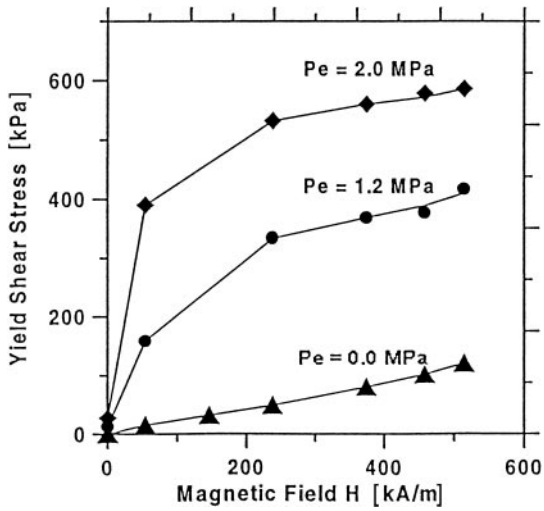

Fig. 7. Yield stress versus magnetic field with and without compression.

$$\tau_{y(H)} = \tau_0 + K_h P_e \quad (2)$$

where τ_0 is the yield stress of the MR fluid without compression. The slope K_h increases with the field H, from 0.221 for H = 238 kA m^{-1}, 0.239 for H = 372 kA m^{-1}, to 0.267 for H = 458 kA m^{-1}. The relationship in Eq. (2) holds for test bars of different sizes. With a small test bar, a static yield shear stress exceeding 800 kPa is obtained. As shown in Fig. 6, the increase of yield stress with the compression force is linear, and there is no sign of saturation. The point of saturation is beyond the capacity of the current measurement.

Figure 7 shows the effect of the magnetic field on the yield stress. The MR fluid without compression has a yield shear stress around 80 kPa at H = 372 kA m^{-1} and 120 kPa at H = 514 kA m^{-1}. The other two curves of the compressed MR fluid were obtained as follows. A magnetic field of 372 kA m^{-1} was first applied, then the MR fluid was compressed with a normal stress of 1.2 MPa or 2.0 MPa, respectively. Then, the coil current was varied and the pullout force was measured at various magnetic fields. During the experiment, at least 30 s was allowed for the MR fluid to relax after the compression or change of magnetic field. Figure 7 clearly indicates that the yield stress is greatly enhanced by the compression. Reducing the magnetic field below 50 kA m^{-1} after the compression led to a sharp drop in the yield stress.

The internal pressure inside the MR fluid is not uniform under compression. During the experiment, the pressure on the test bar was monitored at its midpoint. It is noted that the build-up of pressure under compression was also reduced at low fields as the yield stress dropped. When the magnetic field was off, the MR fluid had a residual yield stress of 20–40 kPa and a residual magnetic field of less than 0.5 kA m^{-1}. This hysteresis indicates that the magnetic particles formed a solid structure under compression and the solid structure remained after the external field was removed. However, the hysteresis was so weak that a light stir returned the MR fluid back to its liquid state immediately.

Figure 8 shows the relationship between the shear stress and the shear strain. The magnetic field was 372 kA m^{-1} for all cases. Without compression, the MR fluid began to yield at a shear stress of 20 kPa. The elastic modulus was about 10^7 Pa. After the yield point, the shear stress increases gradually until it reaches a maximum of 80 kPa at a shear strain of 0.035. With the compression, the MR fluid became much stronger and more rigid. The elastic limit, the modulus, and the yield stress were all increased dramatically. An overshoot of shear stress occurred at a high compression, indicating that the yielding process is sensitive to a structural change. A large shear strain breaks the microstructure of the MR fluid and leads to a sharp decrease of shear stress. At Pe = 2.0 MPa, the shear modulus is as high as 5.0×10^8 Pa, which is 2% of the shear modulus of aluminium. It is also worth mentioning that the structure-enhanced strength of MR fluids is very

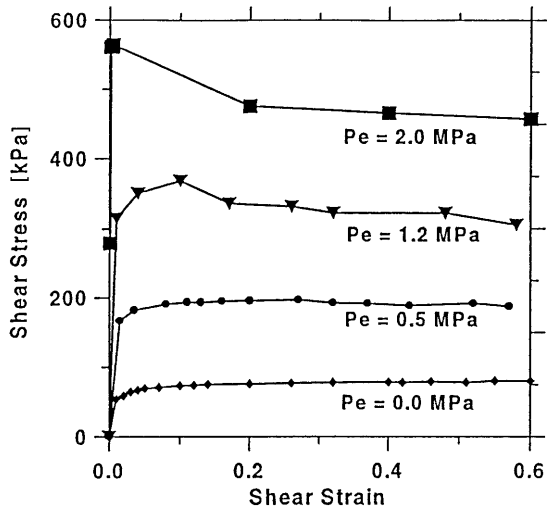

Fig. 8. The relationship of shear stress and shear strain with and without compression.

stable. The shear modulus does not change in 24 h after the compression, as long as the magnetic field holds the fluid.

From the rise in fluid level caused by moving the wedges down, it was noted that the fluid showed a small compressibility. This is because there were some air bubbles in the MR fluid. A vacuum pump was used to extract air bubbles from the MR fluids before the experiment. This made the experiment repeatable. However, it was impossible to remove all the air bubbles. The maximum compressibility ratio of the fluid was 1.5% when the fluid was compressed at $H = 372$ kA m^{-1} at a pressure of 2.0 MPa. Figure 8 shows the relationship between the compression depth and the rise in fluid level. If the fluid is incompressible, the relationship between the compression depth of the sliding plates, δ_s, and the risen MR fluid level, δ_{MR}, is given by

$$\delta_{MR} = L_1\delta_s\tan(\theta)/(L_0 - \delta_s\tan\theta - A_b/L_2) + (L_3 + \delta_s\tan\theta)\delta_s/L_0 - \delta_s\tan\theta - A_b/L_2) \quad (3)$$

where θ is the angle of the guiding plate with respect to the vertical plane. L_0, L_1, L_2, and L_3 are all measurable geometric parameters. The solid line in Fig. 8 is the result of Eq. (3). However, the experimental result deviates from the solid line. This indicates that there were micro air bubbles inside the MR fluid, despite the use of the vacuum technique to extract air bubbles from the MR fluid before the experiment. When the fluid was compressed, there were still some bubbles released. The maximum compressibility ratio of the fluid, $\delta V/V = 1.5\%$, occurred when the fluid was compressed at coil current of 5 A and torque of 5 kg m.

4. Microstructure

To understand the physical mechanism underlying this yield stress enhancement, the microstructure of MR fluid was examined before and after the compression. To do this, instead of silicon oil, polymer resins were used, mixed with iron particles at 45% volume fraction. Then, a magnetic field of 372 kA m^{-1} was applied to the new irreversible MR fluid. The resin had 1 h cure time. In one process, the fluid was not compressed and resin solidified. In another process, the MR fluid was compressed with a pressure of 1.2 MPa and the resin solidified under pressure. Afterwards, the cured solid pieces were cut by a diamond saw and an SEM analysis was conducted. Figure 9(*a*) shows the microstructure of the MR fluid without compression. It is clear that without compression, the microstructure of the MR fluid was a single-chain-dominated structure. As the particles were not uniform, the chains were not perfect, but all of them were not very thick. As shown in Fig. 9(*b*), the MR fluid's microstructure was changed into thick columns

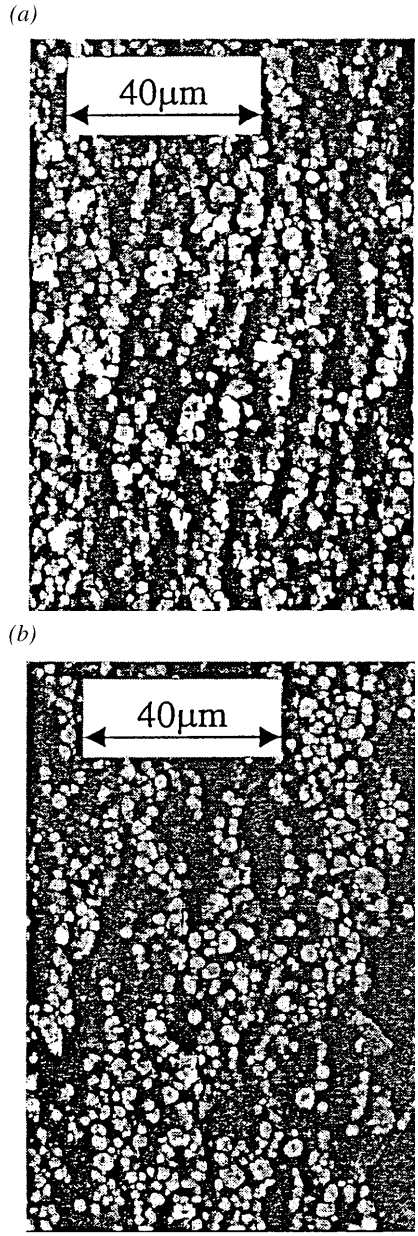

Fig. 9. SEM images of iron-epoxy mixtures cured under magnetic fields (*a*) without and (*b*) with compression.

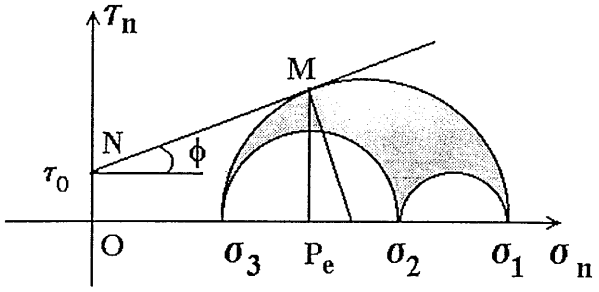

Fig. 10. Mohr-circle diagram to find the limiting stress.

after the compression. The average column thickness was over 50 μm, implying that one column had at least 100 particles or more in its cross-section. When a magnetic field is applied, magnetic particles quickly form chains. Natural aggregation from single chains to thick columns is not only slow, but also produces columns with very limited thickness. When compressing the MR fluid, the chains become shorter and are pushed closer to form a close-packed structure, which is probably a BCT-lattice based structure, having a much higher yield stress and modulus. The columns produced by compression are thicker and stronger than those produced by natural aggregation.

The microstructure is the key to the enhancement of yield stress. In another experiment, the process order was changed: the MR fluid was compressed before application of the magnetic field. Such a process does not produce any yield stress enhancement. The reason is easy to understand. Before the application of a magnetic field, the magnetic particles can move freely within the base liquid. Compression before the formation of a solid structure does not create thick columns. Therefore, there is no change of yield stress.

Once the solid structure is formed in the MR fluid, the normal pressure is no longer uniform within the fluid. The compression thus also increases the friction between the MR particles and the surface of the test bar as the friction is proportional to the normal pressure. It is noted that the yield stress of the compressed MR fluid has a short drop as the magnetic field is reduced below 50 kA m^{-1}. This may also be due to the non-uniform internal pressure. During the compression, close-packed structures are formed and the local internal pressure difference is also increased. When the magnetic field is reduced to a value below 50 kA m^{-1}, the magnetic force is no longer sufficient to resist the local pressure difference, and the particles begin to move to rearrange themselves. The experiment thus also recorded a sharp decrease of the normal stress. This causes a sharp decrease of the yield stress.

5. Discussion

Finally, the empirical Eq. (2) is consistent with the Mohr–Coulomb theory [22,23]. Coulomb first showed that the yield shear stress should linearly increase with the normal stress. Let the MR fluid's stress tensor be denoted by τ_{ij} (i, j = 1, 2, 3), that is, a combination of the mechanical tensor and the Maxwell tensor [24]. The normal stress σ_n and shear stress τ_n on the plane with a normal direction n are given as follows.

$$\sigma_n = \Sigma_{ij}\ \tau_{ij}\ n_i\ n_j \tag{4}$$

$$\sigma_{n2} + \tau_{n2} = \Sigma_{ij1}\ \tau_{ij}\ \tau_{i1}\ n_j n_1 \tag{5}$$

If τ_{ij} has three principal values, $\sigma_1 \geq \sigma_2 \geq \sigma_3$, and the three components of the unit vector n on the three principal axes are still denoted by n_i (i = 1, 2, 3), then Eqs (4) and (5) can be written as,

$$\sigma_n = \sigma_1 n_{12} + \sigma_2 n_{22} + \sigma_3\, n_{32} \tag{6}$$

$$\sigma_{n2} + \tau_{n2} = \sigma_{12}\, n_{12} + \sigma_{22}\, n_{22} + \sigma_{32} n_{32} \tag{7}$$

If the points $(\sigma_2 + \sigma_3)/2$, $(\sigma_1 + \sigma_3)/2$, $(\sigma_1 + \sigma_2)/2$ are used as the centres and $(\sigma_2 - \sigma_3)/2$, $(\sigma_1 - \sigma_3)/2$, $(\sigma_1 - \sigma_2)/2$ as the radii for Mohr circles (Fig. 10), the area confined by the large and two small circles defines all possible values of σ_n and τ_n. As mentioned before, τ_0 is the yield stress without compression, represented by *ON*. The maximum allowed value of τ_n is represented by a point *M*, where the line *NM* is tangential to the largest circle. Hence, the maximum shear stress τ_y is approximately expressed by,

$$\tau_y = \tau_0 + \sigma_n \tan \phi \tag{8}$$

Also from Coulomb, ϕ is the angle of internal friction. If P_e in Eq. (2) is σ_n, then, for example, $\tan\phi = K_h = 0.239$ or $\phi = 13.44°$ at H = 372 kA m^{-1}. The values of ϕ and the internal friction coefficient $\tan\phi$ seem to be reasonable. As mentioned before, K_h increases slightly with the magnetic field. Then the internal friction seems to increase slightly with the magnetic field.

The test bar in the experiment is made of non-magnetic material (aluminium alloy). The "wall effect" may underestimate the yield stress of MR fluid [25, 26]. However, the average MR particles size of 5 μm (Fig. 3) is much smaller than the surface roughness of the bar (~30 μm). There is no reason to believe that the MR particles could slip on the surface. To verify this, an experiment was also conducted with a steel bar. There was no significant change in the results of yield stress. However, it is very difficult to align a steel bar in a high magnetic field. For future applications, it is decided to use an aluminium bar throughout the experiments.

6. Summary

MR fluid is studied experimentally for potential applications in flexible fixturing. A compression technique is applied to increase the yield strength of MR fluids in solid state significantly. A high shear strength of 800 kPa has been achieved, which could be even higher if the test conditions are improved. It is also expected that this compression technique can be used for ER fluids. The study will be continued to develop a fixture design and implementation method for applying MR (or ER) fluids in flexible fixturing.

Acknowledgement

We wish to thank R. Cybert, T. Essery and J. Yu for their assistance. This research is supported by NSF grant SGER-9725012, NNSFC grant 19772049 and a grant from MTC of SIUC.

References

1. J. C. Trappey and C. R. Liu, "A literature survey of fixture-design automation", International Journal of Advanced Manufacturing Technology, 5(3), pp. 240–255, 1990.
2. Y. Rong, S. Li and Y. Bai, "Development of flexible fixturing technique in manufacturing industry", 5th International Symposium on Robotics and Manufacturing, Maui, HI, 15–17 August 1994.
3. Y. C. Chou, R. A. Srinvas and A. Banerjee, "Automatic design of machining fixtures", The NSF Design and Manufacturing Systems Conference, Atlanta, GA, Jan. 1992, pp. 991–994.
4. Y. Zhu and Y. Rong, "A computer-aided fixture design system for modular fixture assembly", Quality Assurance Through Integration of Manufacturing Processes and Systems, ASME WAM, Anaheim, CA, 8–13 November 1992, PED- 56, pp. 165–174, 1992.
5. P. M. Grippo, B. S. Thompson and M. V. Gandhi, "A review of flexible fixturing systems for computer-integrated manufacturing", International Journal of Computer-Integrated Manufacturing, 1(2), pp. 124–135, 1988.
6. B. S. Thompson and M.V. Gandhi, "Commentary on Flexible Fixturing", Applied Mechanics Review, 39(9), pp. 1365–1369, 1986.
7. F. B. Hazen and P. K. Wright, "Workholding automation: innovations in analysis, design, and planning", Manufacturing Review, 43(4), pp. 224–237, 1990.
8. J. Abou-Hanna, K. Okamura and T. McGreevy, "Dynamic behavior and creep characteristics of flexible particulate bed fixtures", Journal of Manufacturing Systems, 12(6), pp. 496–505, 1993.
9. N. Lange, M. V. Gandhi, B. S. Thompson and D. J. Desal, "An experimental evaluation of the capability of a fluidized-bed fixture system", International Journal of Advanced Manufacturing Technology, 4(4), pp. 192–206, 1989.
10. D. A. Brooks, "Electrorheological devices", Chartered Mechanical Engineering, 29(9), pp. 92–95, 1982.
11. R. Tao and Q. Jiang, "Simulation of structure formation in an electrorheological fluid", Physical Review Letters, 73(1), pp. 205–208, July 1994.
12. T. Chen, R. N. Zitter and R. Tao, "Laser diffraction determination of the crystalline structure of an electrorheological fluid", Physical Review Letters, 68(16), pp. 2555–2558, April 1992.
13. X. Wu, "Properies and applications of electrorheological fluids and electroset", MS thesis, Southern Illinois University at Carbondale, 1996.
14. W. I. Kordonsky, "Magnetorheological effect as a base of new devices and technologies", Journal of Magnetism and Magnetic Materials, 122, pp. 395–398, 1993.
15. O. Ashour, C. A. Rogers and W. Kordonsky, "Magnetorheological fluids: materials, characterization, and devices", Journal of Intelligent Material Systems and Structures, 7(2), p. 123–130, 1996.
16. J. M. Ginder and L. C. Davis, "Shear stresses in magnetorheological fluids: role of magnetic saturation", Applied Physics Letters, 65(26), p. 3410–3416, 1994.
17. P. P. Phule and J. M. Ginder, "The materials science of field-responsive fluids", MRS Bulletin, 23(8), p. 9, 1998.
18. R. Tao and J. M. Sun, "Three-dimensional structure of induced electrorheological solid", Physical Review Letters, 67, pp. 398–401, 1991.
19. L. Zhou, W. Wen and P. Sheng, "Condensed matter: electronic properties, etc – ground states of magnetorheological fluids", Physical Review Letters, 81(7), p. 1503–1509, 1998.
20. G. L. Gulley and R. Tao, "Static shear stress of electrorheological fluids", Physical Review E, 48, pp. 2744–2751, 1993.
21. X. Tang and H. Conrad, "Quasistatic measurements on a magnetorheological fluid", Journal of Rheology, 40(6), p. 1167–1178, 1996.
22. S. S. Vyalov, Rheological Fundamentals of Soil Mechanics, Elsevier, New York, 1986.
23. J. J. Tuma and M. Abdel-Hady, Engineering Soil Mechanics, Prentice-Hall, NJ, 1973.
24. R. E. Rosensweig, "On magnetorheology and electrorheology as states of unsymmetric stress", Journal of Rheology, 39, p. 179–192, 1995.
25. G. Bossis and E. Lemaire, "Yield stresses in magnetic suspensions", Journal of Rheology, 35(7), p. 1345–1347, 1991.
26. T. Miyamoto and M. Ota, "Mechanism of stress transmission from an electrorheological fluid to the electric plates", Applied Physics Letters, 64, p. 1165–1170, 1994.